Equilibrium Modelling of CO_2-Brine Systems for Geological Carbon Storage Applications; Experimental Measurements and Thermodynamic Modelling

Sepideh Alimohammadi[1], *Lucky* Abiashue[1], *Babatunde S.* Adigun[1], *Peng* Zhou[1], *Gideon* Nyame[1], *Abdulazeez* Babatunde[1], *Omidreza* Mohammadzadeh[2], and *Lesley A.* James[1*]

[1]Department of Process Engineering, Memorial University of Newfoundland, St. John's, Canada
[2]Department of Petroleum Engineering, University of Alaska Fairbanks, Fairbanks, Alaska

Abstract. The thermodynamic properties of CO2–brine fluid system play a critical role in optimal geological carbon storage (GCS), particularly in saline aquifers. Dissolving CO2 in brine increases storage capacity, but it also causes brine acidity, which could compromise the containment integrity of the storage site. Precise modelling of mutual solubility parameter in CO2-brine system under in-situ reservoir conditions is required to estimate storage efficiency and potential risks associated with CO2 storage in saline aquifers. Traditional cubic equations of state (EoS) struggle to accurately predict water-CO2 interactions due to their inability to account for dipole-dipole and quadrupole-quadrupole forces, which are fundamental in polar fluid systems. To address this limitation, this study employs an extended SRK-Polar equation of state (EoS) integrated with Pitzer-Debye-Hückel method (e-SRK-P) to incorporate electrolyte interactions . By capturing the role of polar interactions between water and CO2, this approach enhances physical consistency of solubility predictions, phase equilibria, and brine acidification under subsurface storage conditions. Unlike conventional models, this framework simplifies electrolyte contributions while ensuring greater accuracy in predicting CO2 behaviour in saline environments. This research presents application of an advanced thermodynamic model to predict CO2 equilibrium in NaCl solution over a range of temperatures (353 -433 k), pressures (up to 124 bar), and salinity (1 - 4 M). A systematic procedure was developed in this study to reliably generate equilibrated CO2-saline water solutions and consistently measure solubility data, which was then used to generate an in-house dataset for model validation. Experimental solubility measurements were conducted using both the direct weighing of the fluid sample and water column displacement techniques to ensure robustness and accuracy. In addition, some CO2-in-brine solubility data over a wider range of conditions were borrowed from the literature. Another renowned model, known as Duan's EoS, was also used for solubility computations, and the results were compared against e-SRK-P EoS predictions for further validation. Compared to the existing EoS modelling techniques, the proposed EoS model demonstrates improved accuracy in predicting CO2 equilibrium concentrations in saline solutions, when compared with the experimental data, with lower Absolute Average Deviations (AADs) of 2.5%. This study contributes to the development of a more reliable predictive tool for CO2-brine interactions, enhancing the effectiveness of GCS strategies, particularly CO2 entrapment through "dissolution in brine" mechanism. By improving the accuracy of CO2 solubility predictions, this work supports better risk assessment and optimization of the GCS operations.

1 Introduction

Despite international climate commitments such as the Paris Agreement, global carbon dioxide (CO_2) emissions remain high. This ongoing challenge has intensified efforts to implement low-carbon technologies across various sectors, including power generation, manufacturing, and energy-intensive industries [1, 2]. Among the most promising approaches is Carbon Capture and Storage (CCS), which involves capturing CO_2 emissions at their source and securely storing them underground within rock pore space. Besides mitigation, geological carbon storage (GCS) is viewed as a large-scale solution to carbon emissions. To effectively design and optimize GCS operations, a comprehensive understanding of CO_2 behaviour under reservoir conditions is essential—particularly its thermodynamic interactions with formation fluids [3, 4, 5].

Solubility trapping is a key trapping mechanism in GCS, where the injected CO_2 dissolves into the formation brine. This process not only enhances long-term storage security by reducing the mobile CO_2 phase but it also initiates important geophysical and geochemical changes

* Corresponding author: ljames@mun.ca

within the subsurface environment. Dissolved CO_2 increases brine density, setting up a gravitational instability that can trigger convective mixing and promote further dissolution. Over time, this interaction influences the extent of CO_2 migration, its chemical reactivity with reservoir minerals due to the lowering of the water pH and formation of carbonic acid, and the overall trapping efficiency [6, 7, 8]. Accurate prediction of mutual solubility between CO_2 and brine is thus fundamental for assessing storage capacity, simulating long-term behaviour, and evaluating potential risks associated with leakage or mineral scaling.

Accurately characterizing CO_2 solubility in brine remains a complex task primarily due to the influence of high ionic concentrations, which significantly alter fluid-phase behaviour and non-ideal interactions. While pressure, temperature, and salinity variations require local calibration, the core thermodynamic challenge lies in representing strong electrolyte effects and polar interactions within the brine. Factors such as salinity, temperature, pressure, and brine composition all influence CO_2 solubility. However, many existing studies rely on simplified synthetic brines and are limited to narrow ranges of operating conditions, particularly with respect to temperature, pressure, and salinity. These synthetic brines typically contain only NaCl, whereas natural formation brines often include a broader spectrum of dissolved ions (e.g., Ca^{2+}, Mg^{2+}, SO_4^{2-}) that can influence fluid phase behaviour and activity coefficients. The lack of comprehensive studies under representative aquifer conditions using consistent and reproducible protocols introduces uncertainty into solubility modelling and its extrapolation to field-scale scenarios. This gap in experimental inconsistency, coupled with limitations in conventional models to capture the thermodynamic behaviour of electrolyte-rich systems, underscores the need for improved data quality and more physically grounded modelling frameworks to support reliable predictions of CO_2 behaviour in geological storage settings [9, 10].

The CO_2–H_2O binary system displays a vapor–liquid–liquid equilibrium (VLLE) curve with a metastable VLLE region. This intricate phase behaviour allows the mutual solubility of CO_2 and H_2O to be studied across a broad temperature and pressure range. Extensive experimental data have been compiled, including those by IUPAC and subsequent studies, leading to the development of several models for solubility prediction. These include φ–φ (EOS–EOS) [11], γ–φ (activity coefficient–EOS) [12, 13, 14], extended Henry's law approaches (e.g., Krichevsky–Kasarnovsky) [15], empirical correlations [19], and, more recently, machine learning methods—each differing in complexity, scope, and underlying assumptions. Traditional cubic equations of state (e.g., Peng–Robinson (PR), Soave–Redlich–Kwong (SRK)) typically model only CO_2 or CO_2–H_2O equilibria, neglecting the presence and effects of dissolved ions. This omission limits their predictive accuracy for brine systems, where ionic strength significantly alters phase behaviour. To address this, γ–φ approaches incorporate activity coefficient models (e.g., Pitzer) that account for ion-specific interactions. More advanced EOS frameworks, such as polar or electrolyte-based models (e.g., e-SRK-P), integrate water's polarity and electrostatic contributions. These enhancements not only improve CO_2 solubility predictions in saline environments but also enable more accurate estimation of secondary properties such as brine–CO_2 mixture density and phase equilibria under subsurface storage conditions [12, 13].

Numerous models have been developed to represent CO_2 solubility in brine systems, often using the γ–φ framework where an activity coefficient model accounts for electrolyte effects. Strong electrolytes are known to reduce CO_2 solubility—a phenomenon typically captured using models like Pitzer, which remains effective across a broad range of ionic strengths. Duan and Sun [14] proposed a widely used model combining an equation of state for the CO_2-rich phase with a simplified Pitzer formulation for common ions, demonstrating broad applicability over a wide range of temperatures, pressures, and salinities, though it does not account for water solubility in the CO_2-rich phase. Subsequent refinements replaced the EoS with empirical expressions to enhance low-temperature accuracy. Similarly, Spycher and Pruess [16] developed a γ–φ model incorporating a modified Redlich–Kwong EoS and activity models for salts, extending applicability up to 573 K, though the model lacks ion-specific distinctions and uses separate formulations for different temperature ranges. More recent efforts, such as the model by Sun *et al.* [17], offer wide-ranging empirical correlations for various ions with good agreement to experimental data. Despite these advances, many models remain limited in scope or rely on simplifications that may overlook critical phase behaviour nuances, particularly under ionic strength.

Accurate experimental measurement of CO_2 solubility in brine is fundamental for reactive transport modelling and geochemical risk assessment in geological carbon storage (GCS), as it directly influences predictions of carbonic acid formation and long-term storage behaviour. Yan *et al.* [18] provided foundational data by measuring CO_2 solubility in NaCl brines at concentrations of 0, 1, and 5 mol/kg over a pressure range of 5 to 40 MPa and temperatures between 323 K and 413 K. Their work confirmed the salting-out effect where solubility decreases with increasing salinity and established clear pressure and temperature dependencies. Building on this, Liu *et al.* [19] extended the analysis to brines containing different salts, such as KCl and $CaCl_2$ (maximum pressure of 155 bar, maximum temperature of 328 K, and the concentration of the salt was up to 3 mol/kg), further verifying the inverse relationship between salt concentration and CO_2 solubility. These studies highlight the significance of experimental solubility data in validating thermodynamic models and understanding brine-specific effects. However, a notable gap remains in systematically examining the influence of dissolution time on solubility equilibrium, particularly in more chemically complex brine systems. This highlights the need for standardized, best-practice experimental

protocols that ensure complete phase equilibration and enable accurate, reproducible measurements.

While solubility trends—such as its increase with pressure and decrease with temperature and salinity—are well established, significant discrepancies persist across published datasets due to variations in experimental protocols, equilibration durations, and measurement techniques. These inconsistencies are especially problematic when extending solubility predictions to complex formation waters with mixed ionic compositions. Although a wide range of studies have focused on pure water and single-salt systems, data for real-world conditions remain sparse. This highlights the need for standardized experimental practices that can reliably reproduce CO_2 solubility under representative subsurface conditions. In this study, we focus on NaCl brine as a baseline system due to its prevalence and extensive documentation in the literature. However, we recognize that real formation brines often contain multiple ionic species (e.g., Ca^{2+}, Mg^{2+}, SO_4^{2-}), which can further influence solubility and phase behaviour. Future work will extend both the experimental protocols and modelling frameworks developed here to multi-component brine systems to better capture reservoir-relevant complexity. Introducing a best-practice framework that ensures complete phase equilibration and minimizes measurement uncertainty is therefore essential to improve data consistency, support model calibration, and enhance confidence in GCS simulations across scales [20, 21].

Duan and Sun's [14] model has been widely adopted for estimating CO_2 solubility in brine due to its simplicity and acceptable accuracy. However, it remains a semi-empirical polynomial-based approach with limited capacity to capture the full thermodynamic behaviour of the system. It primarily accounts for electrostatic interactions via activity coefficient models but does not explicitly model molecular interactions or phase behaviour beyond solubility—offering little to no predictive insight into density, viscosity, or interfacial phenomena. Additionally, Duan and Sun's [14] model neglects the vapor-phase presence of water, an important factor in accurate equilibrium modelling. To address these limitations, we employed an extended electrostatic-Cubic-Polar (e-SRK-P) EoS, which treats both CO_2 and water as components in both liquid and vapor phases. This formulation allows for a more rigorous phase equilibrium calculation and extends the model's applicability to key properties such as interfacial tension (IFT) and density, thereby enhancing the reliability and utility of the EoS for integrated CO_2 storage and transport simulations. In addition to this broader applicability, the e-SRK-P model demonstrates higher accuracy compared to existing models, including Duan and Sun's [14] model, particularly under conditions relevant to subsurface CO_2 sequestration.

Our goal is, first, to develop an advanced thermodynamic modeling framework for CO_2 solubility in brine by extending the electrostatic Cubic-Plus-Polar (e-SRK-P) equation of state with the Pitzer-Debye-Hückel approach. This model captures both polar and long-range electrostatic interactions, offering improved accuracy in predicting CO_2–brine equilibrium across wide ranges of temperature, pressure, and salinity—especially in electrolyte-rich systems where traditional cubic EoS methods are limited. Second, we aim to establish a best-practice experimental methodology for preparing equilibrated CO_2-saturated brine and quantifying solubility using standardized equilibration and dual validation techniques (mass balance and volume displacement). By integrating this physically consistent modeling approach with high-quality experimental measurements, this study enhances the reliability of CO_2 solubility predictions and supports more accurate risk assessments and optimization strategies in geological carbon storage applications.

2 Methodology

2.1 Thermodynamic Modelling

The thermodynamic modelling of CO_2 solubility in aqueous NaCl brine was performed using the extended SRK-Polar (e-SRK-P) equation of state (EoS). This model integrates polar interactions—such as dipole-dipole, quadrupole-quadrupole, and dipole-quadrupole forces—into a Soave–Redlich–Kwong (SRK) base EoS framework and augments it with electrolyte-specific corrections using the Pitzer-Debye-Hückel (PDH) formalism. The e-SRK-P model is suitable for capturing the non-ideal behaviour of polar systems and ion-containing solutions under high-pressure, high-temperature conditions characteristic of CO_2 geological storage [22].

The residual Helmholtz free energy (A^R) in the e-SRK_P model is defined as:

$$A^R = A^{SRK} + A^{Polar} + A^{PDH} \tag{1}$$

Here, A^{SRK} is the standard contribution from the Soave–Redlich–Kwong (SRK) equation of state, which handles non-polar molecular interactions. A^{Polar} adds corrections for polar interactions that are not captured by the cubic term. A^{PDH} stands for the Pitzer-Debye-Hückel (PDH) in the liquid phase. A^{SRK} and A^{Polar} are defined as [23, 24]:

$$A^{SRK} = nRT\ln\left(\frac{v}{v-b}\right) + \frac{an}{b}\ln\left(\frac{v}{v+b}\right) \tag{2}$$

$$A^{\text{Polar}} = \frac{A_2^{\text{Polar}}}{1 - A_3^{\text{Polar}}/A_2^{\text{Polar}}} \tag{3}$$

In Eq. (2), R is the universal gas constant (8.314 J.K$^{-1}\cdot$ mol^{-1}), T, n, b, and v are temperature (K), total moles number, co-volume parameter ($m^3 \cdot mol^{-1}$), and molar volume ($m^3 \cdot mol^{-1}$), respectively. a is the attractive parameter ($Pa.m^6 \cdot mol^{-2}$). In Eq. (3), A_2^{Polar} and A_3^{Polar} are the second-order and third-order perturbation polar terms, respectively. The polar term takes into account dipole-dipole (A_2^{dd}), dipole-quadrupole

(A_2^{dq}), and quadrupole-quadrupole (A_2^{qq}) interactions. A_3^{Polar} was neglected due to its negligible impact on the equilibrium calculations [25, 26, 27].

$$A_2^{\text{Polar}} = A_2^{dd} + A_2^{dq} + A_2^{qq} \tag{4}$$

where these terms are defined as:

$$\frac{A_2^{dd}}{nRT} = -\frac{\rho N_A^2}{6(RT)^2(4\pi\varepsilon_0)^2}\sum_i\sum_j x_i x_j n_{p_i} n_{p_j} \times \frac{\mu_i\mu_j}{d_{ij}^3} I_6^{HS}(\rho^*) \tag{5}$$

$$\frac{A_2^{dq}}{nRT} = -\frac{\rho N_A^2}{2(RT)^2(4\pi\varepsilon_0)^2}\sum_i\sum_j x_i x_j n_{p_i} n_{q_j} \times \frac{\mu_i^2 Q_j^2}{d_{ij}^5} I_8^{HS}(\rho^*) \tag{6}$$

$$\frac{A_2^{qq}}{nRT} = -\frac{7\rho N_A^2}{10(RT)^2(4\pi\varepsilon_0)^2}\sum_i\sum_j x_i x_j n_{q_i} n_{q_j} \times \frac{Q_i^2 Q_j^2}{d_{ij}^7} I_{10}^{HS}(\rho^*) \tag{7}$$

In Eqs. (5) to (7), Q and μ are experimental quadrupole moment and experimental dipole moment, respectively. n_q, n_p, x, N_A, and ε_0 are number of segments with quadrupolar moments, number of segments with dipolar moments, mole fraction, Avogadro's number and the vacuum permittivity ($8.854188 \times 10^{-12}\ \mathrm{J.C^{-2} \cdot m^{-1}}$). The density, ρ, the segment diameter, d, and the density approximation, $I_k^{HS}(\rho^*)$, by Larsen et al [26] are used in these equations.

The long-range electrostatic interactions due to the presence of ionic species (e.g., Na^+, Cl^-) are handled using the Pitzer-Debye-Hückel (PDH) formulation. The ionic activity coefficients are expressed as [24]:

$$\ln \gamma^{e-SRK-P} = \ln \gamma^{SRK-P} + \ln \gamma^{PDH} \tag{8}$$

where activity coefficients for ion and solvent are calculated as follows:

$$\ln \gamma_{ion}^{PDH} = -0.3910\left(\frac{1000\ \mathrm{g/kg}}{M_s}\right)^{0.5}\left(\frac{2z_{\text{ion}}^2}{14.9}\ln(1 + 14.9I_x^{0.5}) + \frac{z_{ion}^2 I_x^{0.5} - 2I_x^{1.5}}{1 + 14.9I_x^{0.5}}\right) \tag{9}$$

$$\ln \gamma_{\text{solvent}}^{\text{PDH}} = -0.3910\left(\frac{1000\ \mathrm{g/kg}}{M_s}\right)^{0.5}\left(-\frac{2I_X^{1.5}}{1 + 14.9I_x^{0.5}}\right) \tag{10}$$

In Eqs. (9) and (10), M_s is the molecular weight of solvent (water) and I_x is the density approximation [23 24].

2.2 Experimental Methods

A systematic experimental protocol was established to assess the solubility of CO_2 in brine under representative subsurface storage conditions. This involved preparing a synthetic live brine-CO_2 system, homogenization through mechanical rocking, precise sampling under isothermal-isobaric conditions, and solubility determination using two complementary quantification techniques. The experiments were performed at 77°C and 103 bar, mimicking aquifer environments pertinent to CO_2 geological storage.

2.2.1 Brine Preparation

Starting with the simple case, a 4 wt% sodium chloride (NaCl) brine solution was prepared by dissolving 40 g of NaCl in one litre of deionized water. This brine was subsequently degassed using a vacuum pump to eliminate any entrained air before being introduced into the sample chamber of the accumulator. The accumulator itself featured a sealed, floating piston that separated the hydraulic and sample chambers, allowing for independent control of pressure and fluid isolation. To pressurize the system, 700 ml of hydraulic oil was delivered into the hydraulic chamber using an ISCO pump. Finally, carbon dioxide (CO_2) gas was introduced into the brine compartment at an initial pressure of 103 bar under ambient temperature conditions (Figure 1A).

2.2.2 Fluid Mixture Equilibration / Homogenization using Mechanical Rocking

To enhance CO2 dissolution in brine by reaching thermodynamic equilibrium concentration, the accumulator was mounted on a mechanical rocking device that provided continuous agitation. A heating jacket was used to elevate and maintain the system temperature at 77°C using an electronic controller and a thermostat, facilitating thorough mixing of gas and liquid at constant temperature. As the temperature increased, the pressure on the sample side of the accumulator was closely monitored, and additional CO2 was injected as necessary to reach and stabilize 124 bar of gauge pressure on the sample side. To assess the effect of mixing duration on CO2 solubility in brine, the system was equilibrated over three different mixing time intervals of 1, 3, and 5 days. Throughout this period, a back pressure regulator (BPR) was employed, set at 131 bar and connected to the sample side of the accumulator to prevent any gas loss and ensure that equilibrium conditions were consistently maintained (Figure 1B).

2.2.3 Sampling from and Flashing of the Live Brine Phase

At the end of the equilibration period, the accumulator was tilted to facilitate effective phase separation between any excess CO2 (if any is present in the sample side) and live brine. A 50 mL sample cylinder was calibrated by measuring its volume to see if it is the same as the nominal volume marked on the body then securely connected it to the live brine outlet. With a positive pressure applied using an ISCO pump, a live brine sub-sample was then extracted with minimal pressure drop during sample collection. To release the dissolved CO2 from the liquid phase, the collected sub-samples underwent a controlled one-stage flash process by creating more expansion

volume through discharging the DI water in the hydraulic side by opening the outlet valve. This caused the pressure to be reduced to almost atmospheric pressure, allowing the gas phase to evolve from the brine (Figure 2D).

2.2.4 Solubility Measurement

Two methods were employed to quantify CO_2 solubility in brine:

2.2.4a Mass Balance

After the flashing process, the system was left undisturbed at the current pressure of about 10 psi for 20 minutes to allow complete phase separation. A tube connected to the sub-sample cylinder was then submerged in a beaker containing deionized water, enabling visual observation of CO2 gas release through bubbling. Once the bubbling ceased, indicating that all the liberated dissolved gas had been expelled, the remaining degassed brine was retained in the cylinder. To quantify the amount of CO2 originally dissolved, the sample cylinder was weighed both before and after the degassing process, and the difference in mass was used to calculate the CO2 solubility. The separate phase of gas and brine can be seen in Figure 1B.

2.2.4b Volume Displacement

For the volume displacement method in Fig 1, a calibrated water column was integrated into the setup using two three-way valves —one functioning as the inlet and the other as the outlet . Initially, the outlet valve was closed, and the column was filled with deionized water at a controlled flow rate of 5 mL/min and atmospheric pressure using the ISCO pump until completely full. The side of sub-sampling accumulator containing the liberated CO2 gas was then connected to the top of the sealed water column. Upon gradually opening the inlet valve, the liberated CO2 gas displaced the deionized water downwards within the calibrated column. The volume of displaced water at atmospheric pressure and room temperature was, measured with precision, corresponded directly to the volume of CO2 that had been dissolved in the brine sample (Figure 2D).

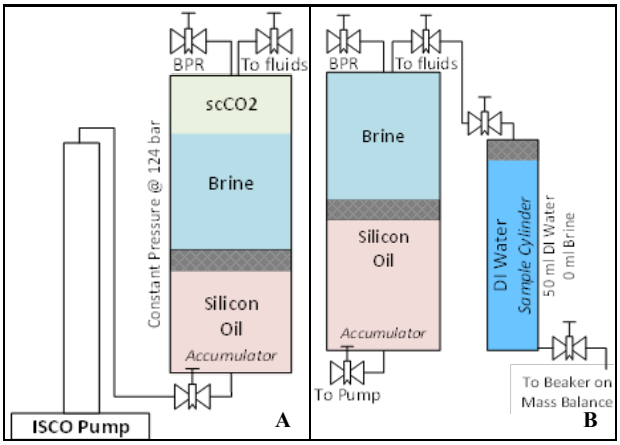

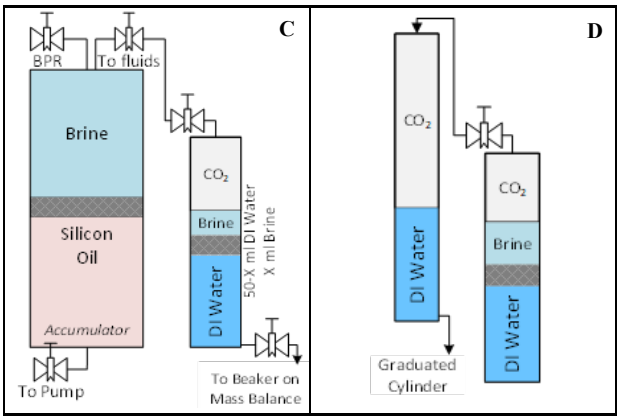

Fig. 1. Schematic diagrams of live brine preparation, sub-sampling, and gas volume measurement system. The diagram illustrates the controlled transfer of live brine under high-pressure and temperature conditions , ensuring accurate solubility measurement through weight and volume displacement methods.

3 Results and Discussions

3.1 Experimental Solubility Measurement

3.1.1 Influence of Rocking Time and Measurement Technique

This research examined the solubility of CO2 in NaCl brine under conditions representative of deep saline aquifers, specifically at 124 bar (1800 psig) and 77°C. It assessed the effect of mixing duration and compared the accuracy of two measurement methods for released CO2 volume measurement: volume displacement and mass balance. A mechanical rocking system was employed to promote mutual solubility interactions between a dead NaCl brine phase and CO2 gas, helping the system reach thermodynamic equilibrium prior to solubility assessment. The findings revealed that achieving thermodynamic equilibrium required more time than initially anticipated, with CO2-in-brine solubility rising from 0.850 mol/kg after one day of rocking to 0.866 mol/kg after five days . The enhanced mixing facilitated by mechanical rocking improves mass transfer at the gas-liquid interface by expanding the interfacial area and inducing convective mixing, thereby accelerating the dissolution process and reducing the dependence on slow molecular diffusion. The observed time-dependent increase in CO2 solubility highlights the critical role of sufficient mixing in attaining thermodynamic equilibrium , as reflected in Table 1 and Figure 2.

Table 1. Standard deviation with experimental methods

Parameter	1 Day	3 Days	5 Days
CO_2 Solubility	0.850	0.857	0.866

(Vol Displacement - mol/kg)			
CO_2 Solubility (Mass Balance - mol/kg)	0.857	0.861	0.869
Average CO_2 Solubility (mol/kg)	0.854	0.859	0.868
Std Deviation (Vol Displacement - mol/kg)	0.0153	0.0154	0.0156
Std Deviation (Mass Balance)	0.0154	0.0155	0.0156

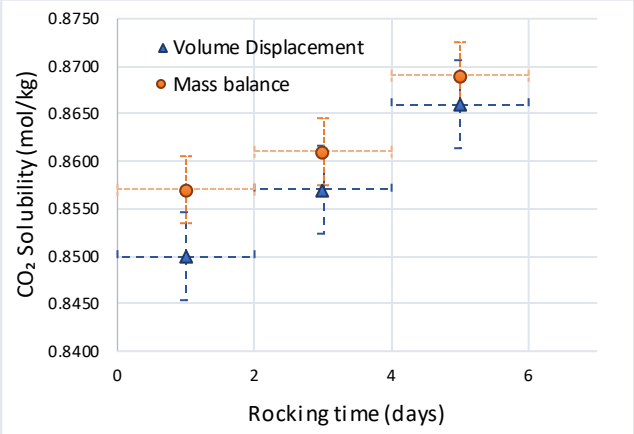

Fig. 2. Influence of mixing duration on CO2 solubility – The graph illustrates how CO2 solubility (in mol/kg) varies with time (in days), comparing results obtained using two measurement techniques: volume displacement (blue) and mass balance (orange).

3.1.2 Validation Against Literature

The experimental results were evaluated against theoretical values predicted by Duan and Sun's [14] model, which combines a custom-developed, parameter-rich equation of state for the CO_2 vapor phase with the Pitzer model for the aqueous phase. In this study, we reprogrammed Duan and Sun's [14] model and independently regenerated solubility data to enable direct comparison with our experimental measurements. For additional validation, experimentally measured CO_2 solubility and brine density data from Yan *et al.* [18] were also referenced. Their study offers a valuable dataset for CO_2–NaCl systems across pressure (up to 400 bar), temperature (140 °C), and salinity range (0–5 mol/kg NaCl), covering our experimental range of interest. However, the scope remains limited to single-salt systems, and their model evaluation focuses primarily on Søreide–Whitson and empirical correlations, which underperform in high salinity scenarios. These constraints highlight the need for broader validation efforts that extend beyond NaCl-only systems and integrate more comprehensive thermodynamic frameworks. As shown in Table 2, the experimental measurements closely match model predictions, particularly after five days of mixing, where the observed solubility (0.869 mol/kg) closely aligns with Duan and Sun's prediction (0.868 mol/kg). Minor differences at shorter mixing durations indicate potential kinetic constraints, such as limited gas-phase mixing or diffusion-related delays in reaching equilibrium. These observations underscore the need to account for mass transfer limitations in practical CO_2 injection scenarios, as insufficient residence time could lead to reduced solubility and lower storage efficiency.

Table 2. Comparison of standard deviation with literature data

Source	Measured CO_2 Solubility - Experimental Avg (mol/kg)	Std Deviation (%) Duan and Sun's Model [14]	Std Deviation (%) Yan et al [18]
Yan *et al.* [18]	**0.863**	-	-
Experiment 5-days rocking	**0.867**	**0**	**0.005**
Experiment 3-days rocking	0.859	0.009	0.004
Experiment 1-day rocking	0.853	0.014	0.009

3.1.3 Sources of Experimental Uncertainty

A number of factors were identified that may contribute to minor inconsistencies in measured solubility values:

- Temperature fluctuations (73–80°C): CO_2 solubility is sensitive to temperature changes, with higher temperatures leading to lower solubility.
- Limited weighing precision: The balance used had only one decimal place, introducing uncertainty in mass-based calculations.
-Gas injection variability: Inconsistencies in the injection process affected the efficiency of gas-liquid contact and mixing.
- Instrumentation and human factors: Minor deviations were introduced through valve operation, manual sample handling, and visual observation.

3.2 Thermodynamic Modelling

In this study, all binary interaction parameters (BIPs) required for e-SRK-P model were sourced directly from literature [22], eliminating the need for further optimization or empirical adjustment. This approach enhances the model's transparency and transferability while maintaining its predictive accuracy. Phase equilibrium calculations were performed under the assumption that water and CO_2 are present in both vapor and liquid phases, whereas the salt (NaCl) is restricted to the liquid phase only, in accordance with physical reality. To manage the complexity inherent in modelling electrolyte systems, polar interactions—including dipole–dipole, quadrupole–quadrupole, and dipole–quadrupole forces—were accounted for only in water and CO_2, and excluded for ionic species. Long-range electrostatic interactions introduced by the dissolved salt were rigorously treated using the Pitzer–Debye–Hückel formalism, which provides a robust thermodynamic foundation for modelling ion-ion and ion-solvent interactions without excessive parameterization.

3.2.1 Comparison of EoS Modelling Results with the Measured Data

Figure 3 and Table 2 compares the measured CO_2 solubility in brine (mol/kg water) after different mixing durations—1, 3, and 5 days with predictions from the e-SRK-P thermodynamic model under constant reservoir-like conditions (124 bar, 77°C, and 4 wt% NaCl). The experimental results show a slight but consistent increase in CO_2 solubility with extended rocking time, indicating that longer equilibration periods promote greater gas dissolution, likely due to enhanced mass transfer at the gas-liquid interface. The measured solubility values ranged from approximately 0.853 to 0.867 mol/kg, demonstrating good reproducibility and clear sensitivity to the duration of mixing.

The e-SRK-P model, used for comparison, slightly underpredicts the solubility data relative to the experimental values, with the modelled value falling within 6% of the measured average after 5 days. This level of agreement is considered satisfactory given the complexity of electrolyte-gas-liquid systems and the sensitivity of solubility to subtle variations in temperature, pressure, and salinity. The small deviation may reflect the model's limitations in accounting for kinetic effects or imperfect phase contact during shorter experiments. Overall, the results support the reliability of the e-SRK-P model under the tested conditions, while reinforcing the importance of allowing sufficient mixing time in laboratory measurements to ensure equilibrium is achieved.

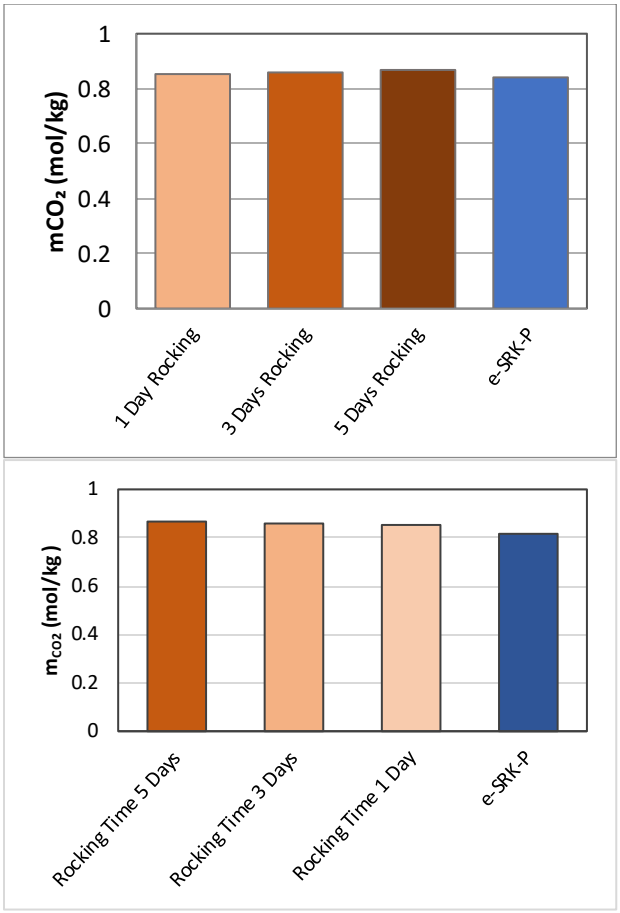

Fig. 3. CO_2 solubility (mol/kg) in NaCl brine after 1, 3, and 5 days of mixing, compared with e-SRK-P model prediction at 124 bar and 350 K (77°C).

3.2.2 Comparison with Duan and Sun [13] Model

Figure 4 illustrates the comparison of CO_2 mole fractions (x_{CO_2}) as a function of pressure for three experimental temperature sets (353, 393, and 433 K) [28], overlaid with predictions from the e-SRK-P model and the well-established Duan and Sun model [14]. As expected, CO_2 solubility increases with pressure and decreases with temperature, aligning with known thermodynamic trends for gas dissolution in saline systems. The plot shows that both models track the experimental data reasonably well across all three temperatures, with slightly better agreement observed at lower temperatures.

To quantify the model performance, the Average Absolute Deviation (AAD%) was calculated between each model and the experimental data. For T = 353 K, Duan and Sun's [13] model shows an AAD of 3.85%, while e-SRK-P performs slightly better with an AAD of 3.14%. At T = 393 K, the AADs are 3.33% (Duan and Sun [13]) and 2.42% (e-SRK-P), again indicating a modest edge for the e-SRK-P model. For T=433 K, both models perform comparably, with AADs of 2.57% (Duan and Sun [13]) and 2.01% (e-SRK-P) (Table 3).

Table 3. AAD% of Duan and Sun [14] and e-SRK-P model's predictions compared to the experimental CO_2 solubility data at selected temperatures.

Temperature (K)	Duan and Sun's [14] Model AAD%	e-SRK-P AAD%
353	3.85	3.14
393	3.33	2.42
433	2.57	2.01

These findings demonstrate that both models are robust within the tested range, but the e-SRK-P model shows a slightly improved predictive capability, especially at higher temperatures. This reflects the advantage of including polar and electrolyte effects explicitly in the e-SRK-P formulation, making it particularly suitable for geological CO_2 storage applications in brine-rich environments.

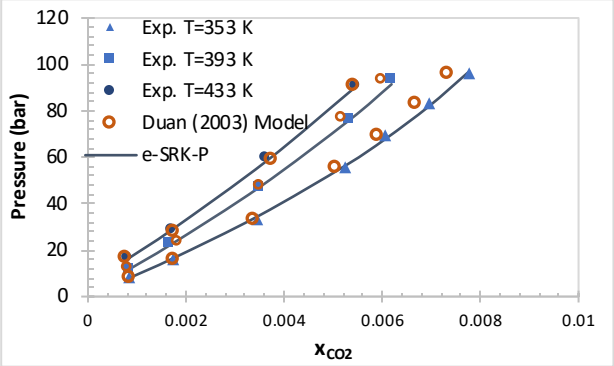

Fig. 4. Comparison of experimental CO_2 solubility data [26] at 353 K, 393 K, and 433 K and NaCl molality of 4 mol/kg with predictions from the e-SRK-P model and the Duan and Sun model [13].

Conclusion

This study introduced a standardized experimental framework for measuring CO2 solubility in brine under conditions representative of deep geological carbon storage (GCS) and evaluated the predictive performance of a physically consistent thermodynamic model to obtain the solubility values. The results confirmed that mixing duration plays a critical role in reaching thermodynamic equilibrium, with both mass balance and volume displacement techniques providing consistent and reproducible measurements.

The extended SRK-Polar (e-SRK-P) model, which explicitly accounts for dipole–dipole, quadrupole–quadrupole, and dipole–quadrupole interactions, as well as long-range electrostatic forces via the Pitzer–Debye–Hückel method, demonstrated superior accuracy in CO2 solubility prediction compared to the widely-used Duan model. While both models aligned reasonably well with the experimental data, the e-SRK-P model consistently achieved lower average absolute deviations (AAD%), particularly at elevated temperatures. Notably, the model used in this study relies exclusively on parameters and binary interaction coefficients sourced from the literature, eliminating the need for extensive data regression and enhancing its general applicability.

Given its strong predictive performance and physical foundation, the e-SRK-P model offers a more efficient and reliable alternative to traditional approaches for simulating CO2–brine phase behaviour. Future work will expand the model's capabilities to predict other key thermodynamic properties—such as interfacial tension (IFT) and fluid density—which are critical for modelling CO2 plume migration, capillary trapping, and reservoir behaviour in long-term GCS scenarios.

References

1. I. Pcc, Climate Change 2021: The Physical Science Basis. Contribution of Working Group I to the Sixth Assessment Report of the Intergovernmental Panel on Climate Change, Cambridge University Press, Cambridge, United Kingdom and New York, NY, USA (2021)
2. G. Peridas, S.B. Mordick, Electr. J. 34, 106996 (2021)
3. H. Wang, B. Li, A. Roy, A. Yousefian, S. Ayirala, Geophys. Res. Lett. 47, e2020GL088490 (2020)
4. H. Wang, V. Alvarado, D.A. Bagdonas, J.F. McLaughlin, J.P. Kaszuba, D. Grana, E. Campbell, K. Ng, Int. J. Greenh. Gas Control 107, 103283 (2021)
5. H. Wang, C. Wang, M. Liu, Z. Deng, Z. Li, H. Bai, J. Bai, Energy 265, 126379 (2023)
6. A. Javaheri, C. Sun, R. Juanes, Fluid Dyn. Mater. Process. 3, 6 (2023)
7. W. Amarasinghe, I. Fjelde, J.Å. Rydland, Y. Guo, Int. J. Greenh. Gas Control 99, 103082 (2020)
8. H. Aydin, S. Akin, Geothermics 113, 102774 (2023)
9. M.F. Irfan, T.M. Bisson, E. Bobicki, F. Arguelles-Vivas, Z. Xu, Q. Liu, et al., Colloids Surf. A Physicochem. Eng. Asp. 548, 37–45 (2018)
10. R.J. Rosenbauer, B. Thomas, Developments and Innovation in Carbon Dioxide (CO_2) Capture and Storage Technology, Woodhead Publishing, 57–103 (2010)
11. F. Tabasinejad, R.G. Moore,S.A. Mehta, K.C.V. Fraassen, Y. Barzin, J.A. Rushing, et al. Ind Eng Chem Res. 50:4029–41 (2011)
12. P. Paricaud, A. Galindo, G. Jackson, Fluid Phase Equilib. 194–197, 87–96 (2002)
13. Z. Khoshraftar, A. Ghaemi, Case Stud. Therm. Eng. 7, 100338 (2023)
14. Z. Duan, R. Sun, Chem. Geol. 193, 257–271 (2003)
15. J. J. Carroll, A. Mather, J Solution Chem. 21(7):607–21 (1992).
16. N. Spycher, K. Pruess, J. Ennis-King, Geochim. Cosmochim. Acta 67, 3015–3031 (2003)
17. X. Sun, Z. Wang, H. Li, H. He, B. Sun, Desalination 504, 114972 (2021)
18. W. Yan, S. Huang, E.H. Stenby, Int. J. Greenh. Gas Control 5, 1460–1477 (2011)
19. Y. Liu, M. Hou, G. Yang, B. Han, J. Supercrit. Fluids 56, 125–129 (2011)

20. L. Steel, Q. Liu, E. Mackay, M. Maroto-Valer, Heriot-Watt Univ. Rep., CO_2 Solubility Measurements in Brine under Reservoir Conditions: A Comparison of Experimental and Geochemical Modelling Methods (2013)
21. A. Shokrollahi, A. Tatar, A. Zeinijahromi, Sustainability 16, 7273 (2024)
22. G.M. Kontogeorgis, G.K. Folas, Thermodynamic Models for Industrial Applications: From Classical and Advanced Mixing Rules to Association Theories, John Wiley & Sons, Ltd., ISBN: 9780470697269 (2010)
23. L. Blum, J.S. Hoeye, J. Phys. Chem. 81, 1311 (1977)
24. K.S. Pitzer, J. Am. Chem. Soc. 102, 2902 (1980)
25. A.J. de Villiers, C.E. Schwarz, A.J. Burger, Fluid Phase Equilib. 312, 66 (2011)
26. B. Larsen, J.C. Rasaiah, G. Stell, Mol. Phys. 33, 987 (1977)
27. R. Shahriari, M.R. Dehghani, B. Behzadi, Fluid Phase Equilib. 313, 60 (2012)
28. B. Rumpf, H. Nicolaisen, C. Ocal, G. Maurer, J. Solution Chem. 23, 431–448 (1994)